

## Supplementary Information

### **Cellulose Dissolution and Encapsulation Strategy to Prepare Carbon Nanospheres with Ultra-Small Size and High Nitrogen Content for Oxygen Reduction Reaction**

Fuping Zhang, Liu Liu, Long Chen, Yulin Shi\*

*School of Chemistry and Chemical Engineering, Key Laboratory for Green Processing  
of Chemical Engineering of Xinjiang Bingtuan, Shihezi University, Shihezi 832003, P.R.  
China.*

\*Corresponding author (Email address: shiyulin521@126.com; Tel.: +86-993-2055030)

## RHE calibration

The calibration was performed CV at a scan rate of 5 mV s<sup>-1</sup> in the high purity H<sub>2</sub>-saturated 0.1 M KOH with a Pt plate (1 cm × 1 cm) as a working electrode, Hg/HgO electrode as a reference electrode, and platinum wire as a counter electrode. The average of the two potentials at which the current density equaled zero was taken to be the thermodynamic potential for the hydrogen electrode reactions (Fig. S1),  $E(\text{vs. RHE}) = E(\text{vs. Hg/HgO}) + 0.896 \text{ V}$ .

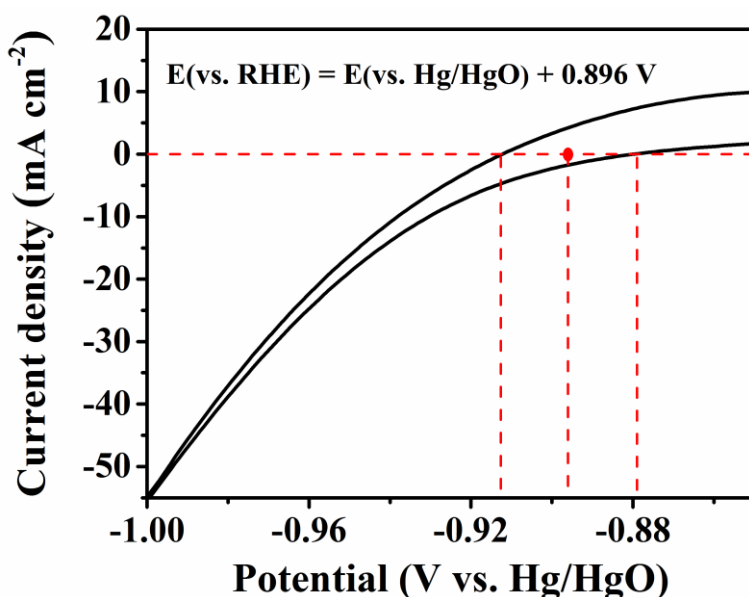


**Fig. S1** Calibration of potentials of the Hg/HgO electrode in 0.1 M KOH to the reverse hydrogen electrode (RHE).

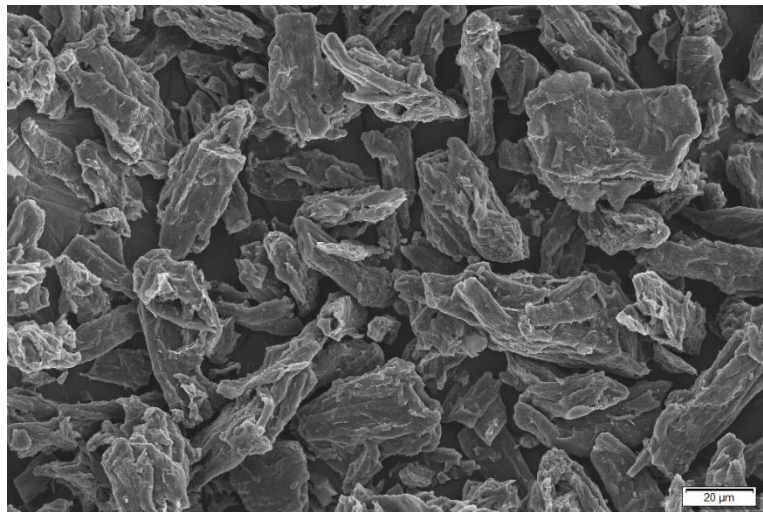


**Fig. S2** SEM image of microcrystalline cellulose directly derived carbon.

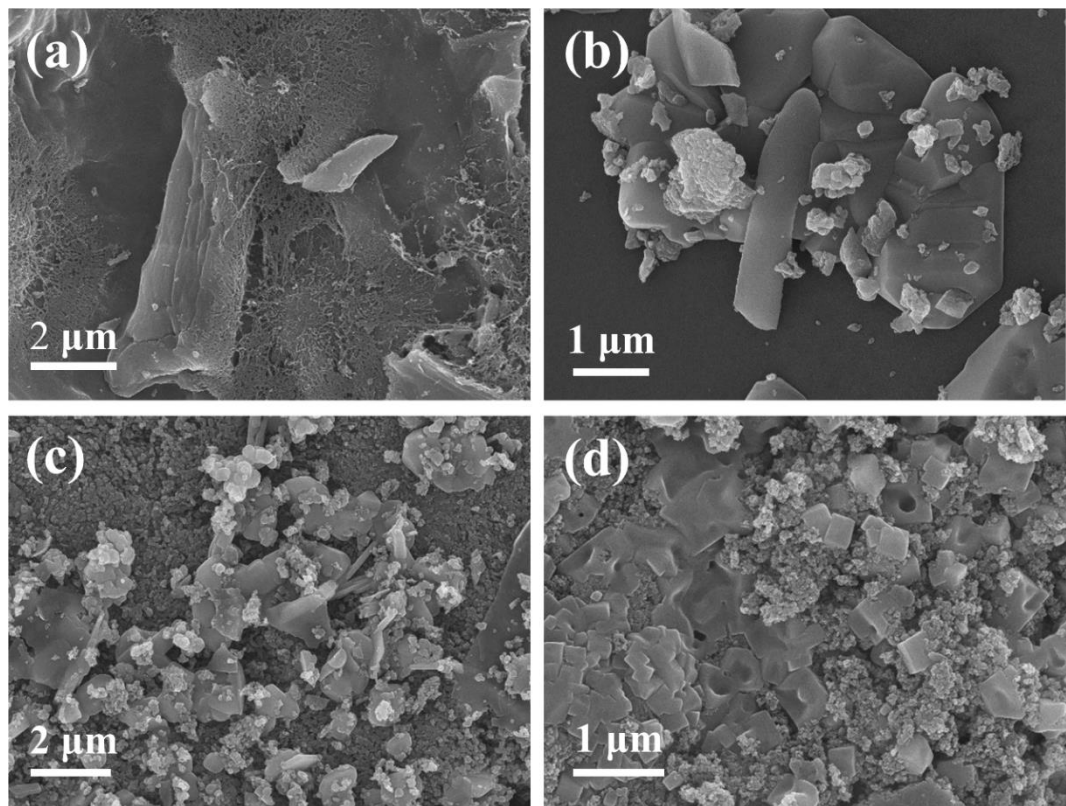


**Fig. S3** SEM images of (a) NCN@ZnCl<sub>2</sub>-0, (b) NCN@ZnCl<sub>2</sub>-2, (c) NCN@ZnCl<sub>2</sub>-3 and (d) NCN@ZnCl<sub>2</sub>-7, respectively.

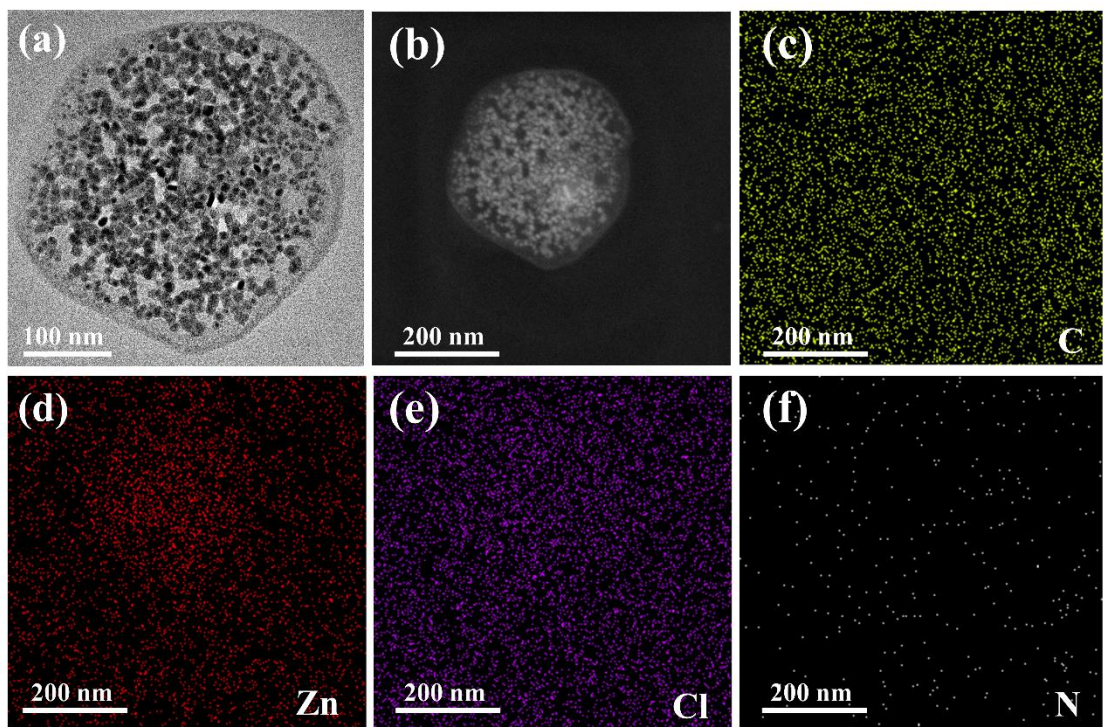


**Fig. S4** TEM image (a), scanning transmission electron microscopy (STEM) image (b) and corresponding C (c), Zn (d), Cl (e), and N (f) elemental mappings of NCN@ZnCl<sub>2</sub>-7 at 500 °C.

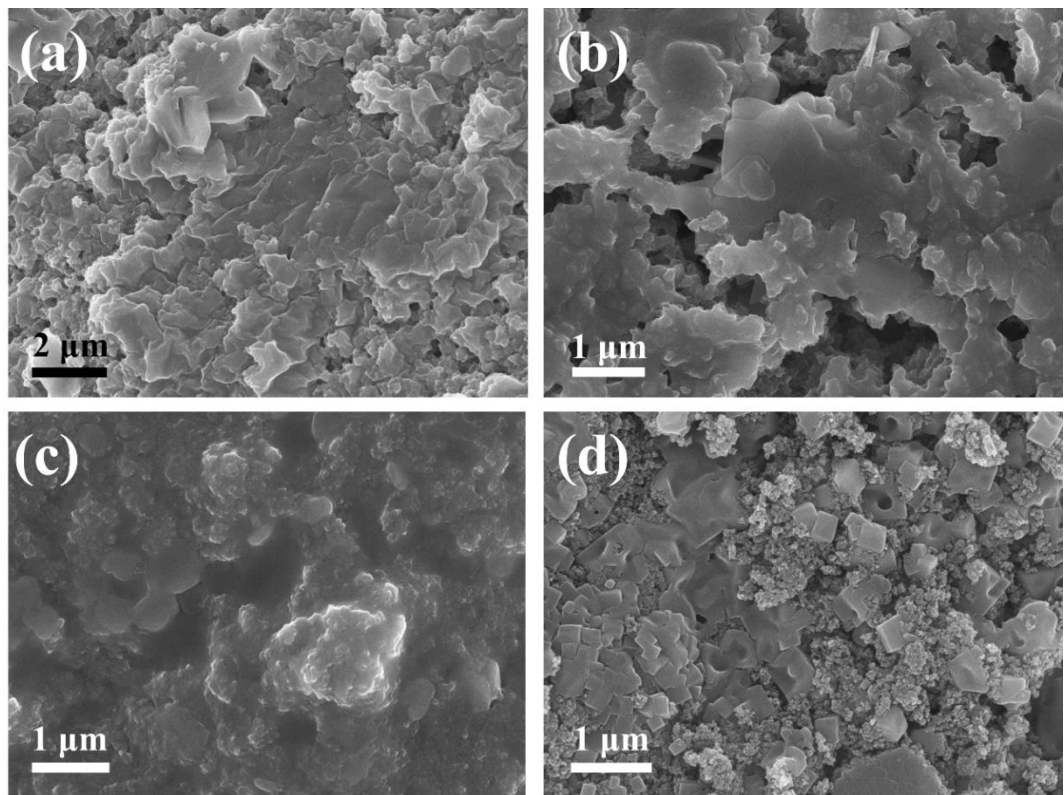


**Fig. S5** SEM images of NCN@ZnCl<sub>2</sub>-7 pyrolysis state: (a) pyrolysis at 500 °C, (b) 600 °C, (c) 700 °C and (d) 800 °C.

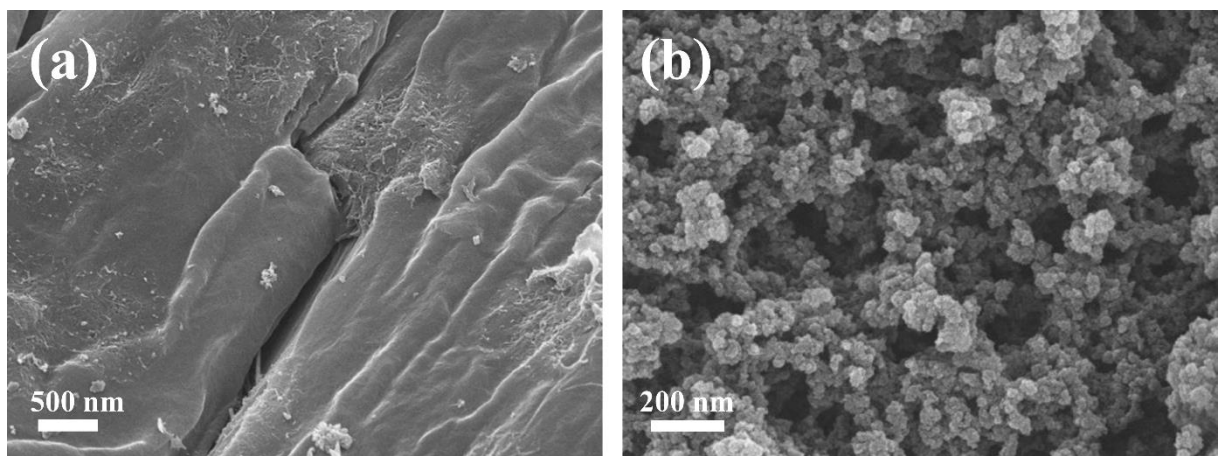


**Fig. S6** SEM images of (a) NCN-0 and (b) NCN-7.

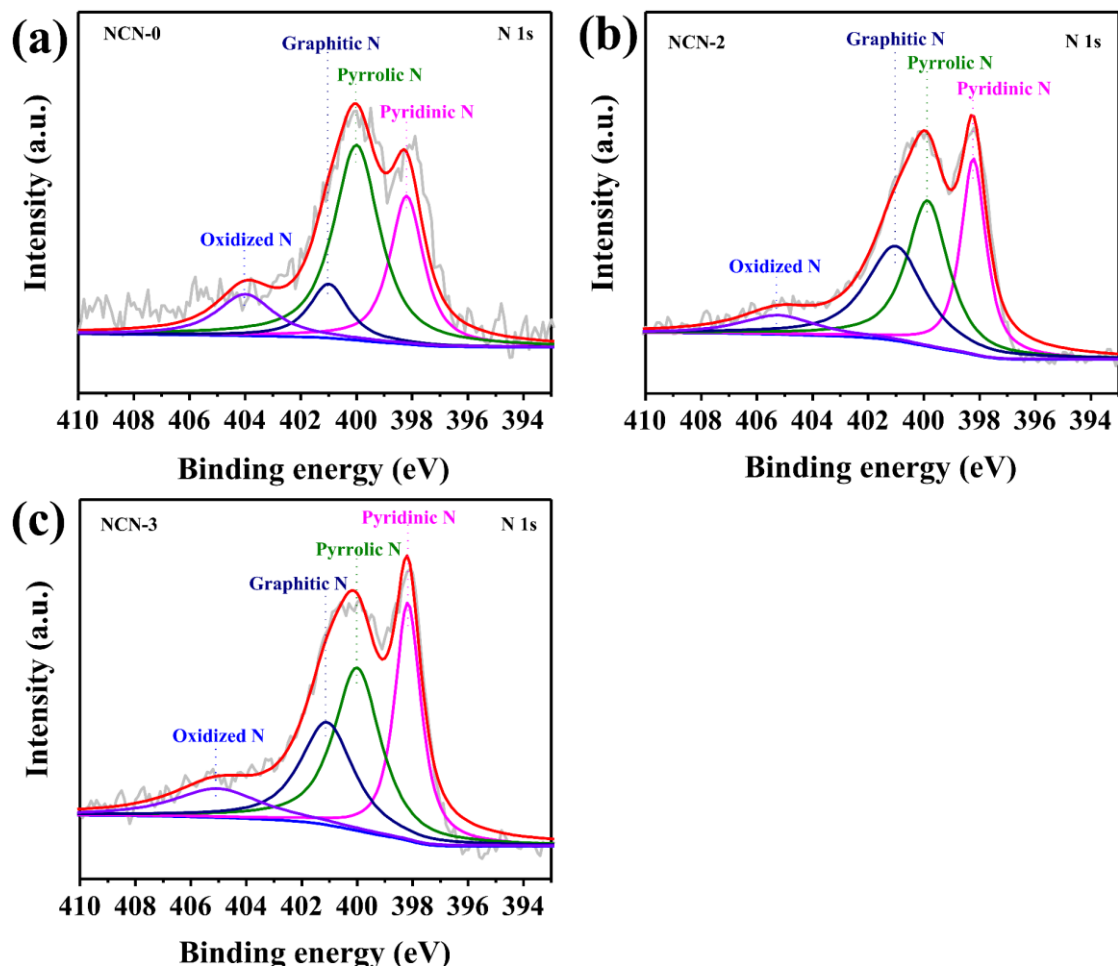


**Fig. S7** High-resolution N 1s XPS spectra of (a) NCN-0, (b) NCN-2 and (c) NCN-3, respectively.

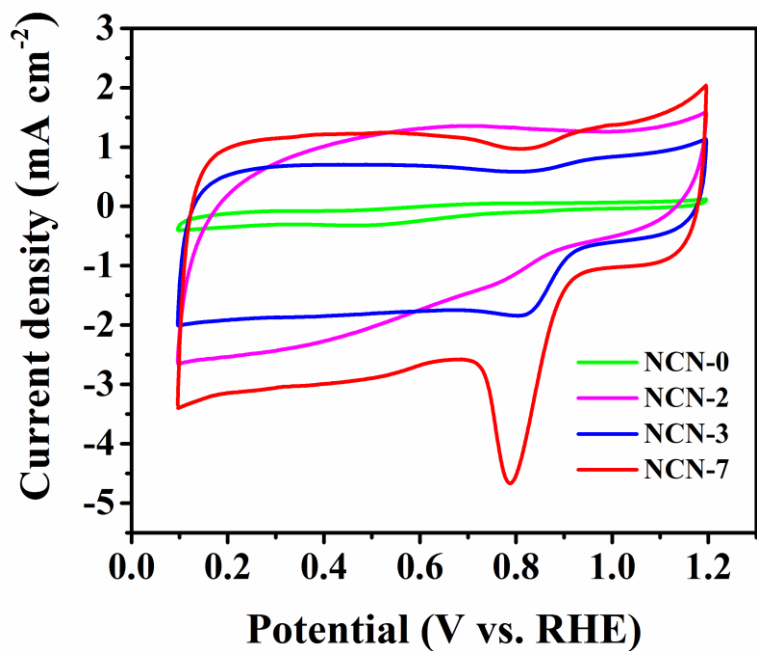


**Fig. S8** Cyclic voltammetry (CV) curves of NCN-X (X=0, 2, 3 and 7) conducted in O<sub>2</sub>-saturated KOH solution with a scan rate of 50 mV s<sup>-1</sup>.

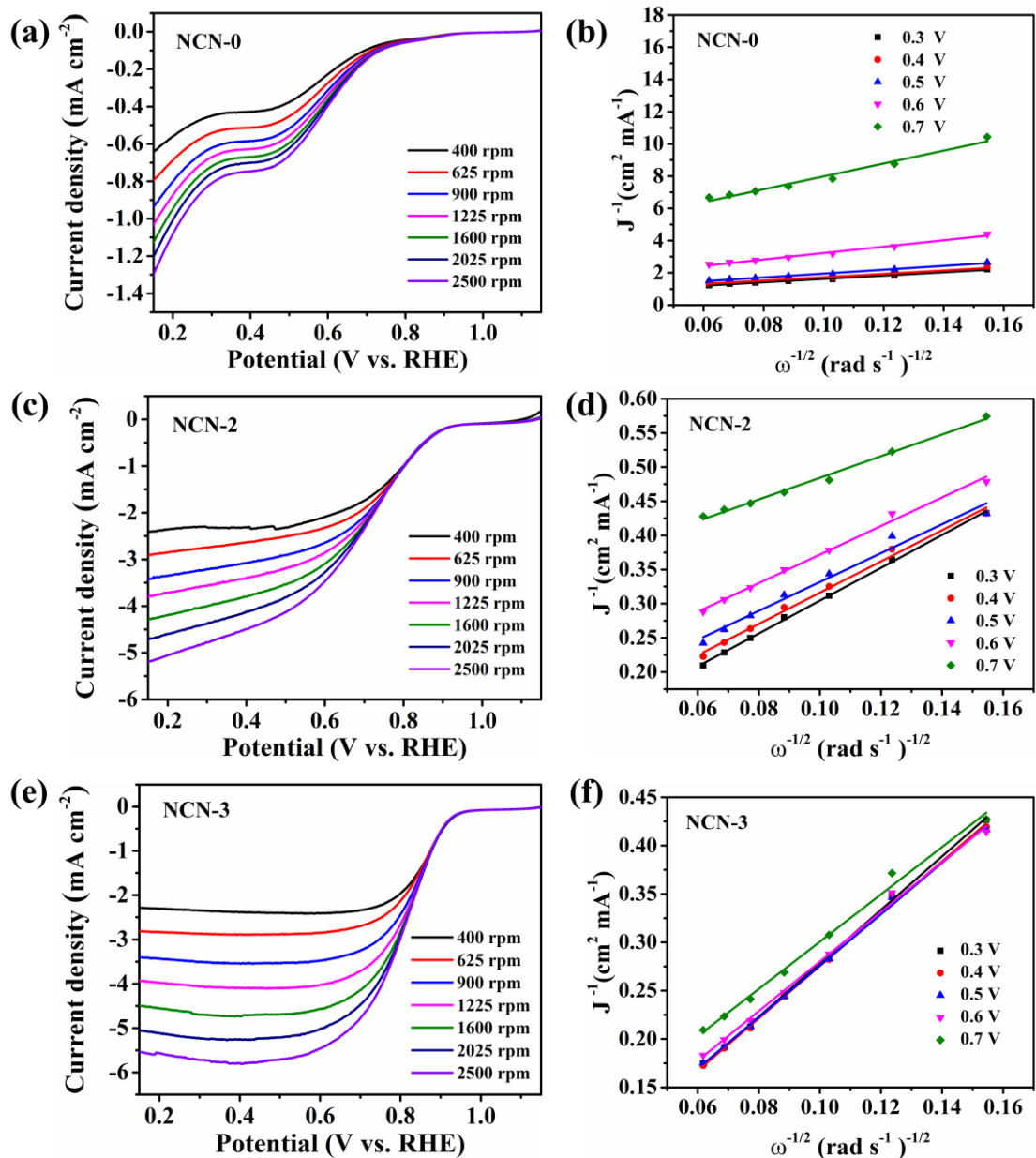


**Fig. S9** (a, c, e) LSV curves and (b, d, f) corresponding K-L plots of (a, b) NCN-0, (c, d) NCN-2, and (e, f) NCN-3 in  $\text{O}_2$ -saturated 0.1 M KOH solution.

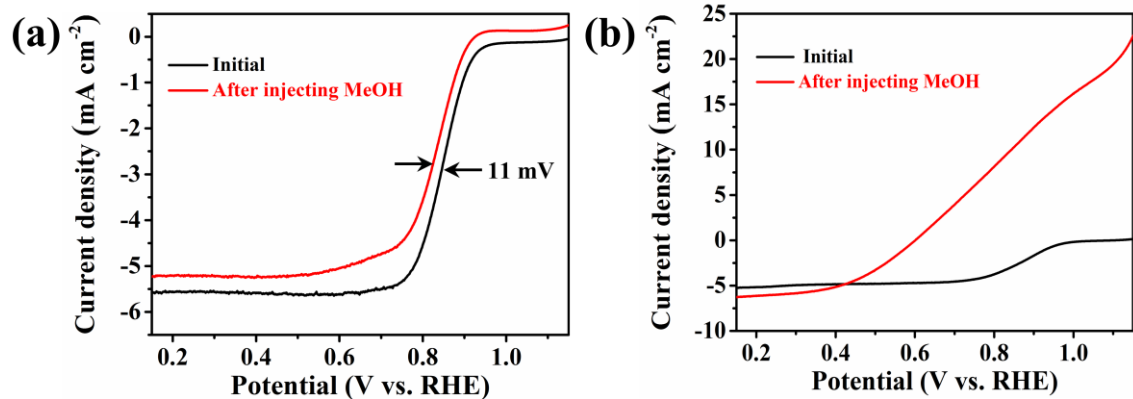


**Fig. S10** LSV curves showing the comparison of NCN-7 (a) and 20% Pt/C (b) for ORR in  $O_2$ -saturated 0.1 M KOH solution with  $5 \text{ mV s}^{-1}$  before (black) and after (red) injecting 10% (volume fraction) methanol.

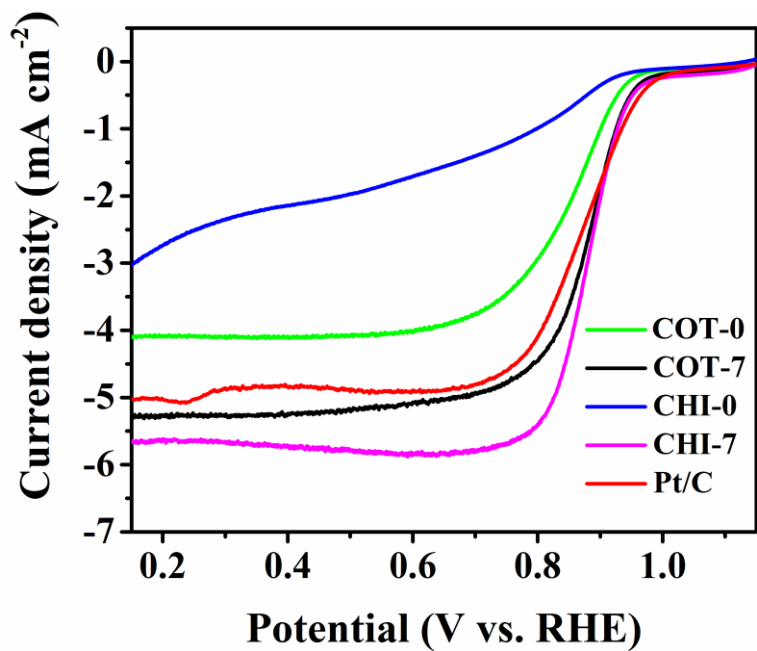


**Fig. S11** LSV curves of CHI-0, CHI-7, COT-0, COT-7 and Pt/C recorded at 1600 rpm in O<sub>2</sub>-saturated 0.1 M KOH solution with the scan rate of 5 mV s<sup>-1</sup>.

**Table S1** Surface atom contents and porous structural characteristics of different samples.

| Sample | C<br>(at.%) | O<br>(at.%) | N<br>(at.%) | Pyridinic<br>N (at. %) | Pyrrolic<br>N (at. %) | Graphitic<br>N (at. %) | Oxidized<br>N (at. %) | S <sub>BET</sub><br>/(m <sup>2</sup> g <sup>-1</sup> ) | S <sub>Micro</sub><br>/(m <sup>2</sup> g <sup>-1</sup> ) | S <sub>meso</sub><br>/(m <sup>2</sup> g <sup>-1</sup> ) | V <sub>Pore</sub><br>/(cm <sup>3</sup> g <sup>-1</sup> ) | V <sub>Micro</sub><br>/(cm <sup>3</sup> g <sup>-1</sup> ) | D <sub>Ave</sub><br>(/nm) |
|--------|-------------|-------------|-------------|------------------------|-----------------------|------------------------|-----------------------|--|--|---|--|---|---------------------------|
| NCN-0  | 68.09       | 27.83       | 4.08        | 1.11                   | 1.99                  | 0.46                   | 0.52                  | 81.0   | 57.6   | 23.4  | 0.061  | 0.032   | 2.99                      |
| NCN-2  | 83.94       | 9.03        | 7.02        | 1.95                   | 2.37                  | 2.16                   | 0.55                  | 1,468.0  | 410.2  | 1057.8  | 0.89   | 0.21  | 2.43                      |
| NCN-3  | 83.9        | 7.13        | 8.97        | 2.59                   | 3.10                  | 2.25                   | 1.03                  | 1,512.3  | 448.7  | 1063.6  | 1.41   | 0.28  | 3.74                      |
| NCN-7  | 85.42       | 6.03        | 8.56        | 3.06                   | 2.33                  | 2.50                   | 0.68                  | 1,655.0  | 163.2  | 1491.8  | 2.08   | 0.10  | 5.03                      |
| CHI-0  | 75.93       | 19.26       | 4.81        | 0.78                   | 1.19                  | 2.09                   | 0.75                  |  |  |   |  |   |                           |
| CHI-7  | 86.17       | 7.96        | 5.87        | 1.52                   | 1.43                  | 1.60                   | 1.32                  |  |  |   |  |   |                           |
| COT-0  | 83.53       | 12.56       | 3.91        | 0.79                   | 1.32                  | 1.14                   | 0.66                  |  |  |   |  |   |                           |
| COT-7  | 85.23       | 9.56        | 5.21        | 1.42                   | 1.27                  | 1.46                   | 1.06                  |  |  |   |  |   |                           |

S<sub>BET</sub>: BET specific surface area, S<sub>Micro</sub>: Micropore surface area, V<sub>Pore</sub>: Pore volume, V<sub>Micro</sub>: Micropore volume, D<sub>Ads</sub>: Adsorption average pore diameter (4V/A by BET).

**Table S2** Comparison of N content and electrocatalytic performances of NCN-7 and biomass-derived carbon materials in other reported work.

| Source of biomass | Materials  | N content /% | Eonset /V | E <sub>1/2</sub> /V | J <sub>L</sub> /(mA cm <sup>-2</sup> ) | Reference   |
|-------------------|--|--------------|-----------|---------------------|--|---|
| Soybean           | Fe/C-SOYB  | 4.95         | 0.84      | 0.68                | 2.6                                    | J. Power Sources, 2014, <b>269</b> , 841-847        |
| Enoki mushroom    | N-C@CNT-900  | 3.2          | 0.94      | 0.81                | 3.98                                   | Nanoscale, 2015, <b>7</b> , 15990-15998             |
| Sodium alginate   | Ni/NiO/NiCo <sub>2</sub> O <sub>4</sub> /N-CNT-As      | 1.2          | 0.89      | 0.74                | ≈4.9                                   | J. Mater. Chem. A, 2016, <b>4</b> , 6376-6384.      |
| Corn silk         | N-P-Fe-C   | 6.55         | 0.957     | 0.852               | ≈5.51                                  | J. Mater. Chem. A, 2016, <b>4</b> , 8602-8609       |
| Filter paper      | FP-Fe-N-850  | 7.32         | 0.98      | ≈8.3                | 5.0                                    | Angew. Chem., Int. Ed., 2016, <b>55</b> , 1355-1359 |
| Lysine            | NCHCs  | 4            | 0.92      | ≈0.80               | ≈6.0                                   | Nanoscale, 2017, <b>9</b> , 1059-1067               |
| Pomelo peel       | PPC-NaZnFe   | 2.92         | -         | 0.86                | ≈5.9                                   | Carbon, 2018, <b>130</b> , 692-700                  |
| Chitosan          | Co <sub>16%</sub> -NCNT-T800                           | 7.61         | -         | 0.835               | 6.92                                   | J. Mater. Chem. A, 2018, <b>6</b> , 5740-5745.      |
| Glucose           | N <sub>0.54</sub> -Z <sub>3</sub> /M <sub>1</sub> -900 | 3.62         | 0.94      | 0.824               | 4.3                                    | Energy Environ. Sci., 2019, <b>12</b> , 648-655     |
| Raw wood          | N/E-HPC-900  | 3.7          | -         | 0.84                | ≈5.9                                   | Adv. Mater., 2019, <b>31</b> , 1900341              |
| Cellulose         | NCN-7  | 8.56         | 0.99      | 0.87                | 5.5                                    | This work   |